WARSAW UNIVERSITY OF TECHNOLOGY Index 351733
FACULTY OF CIVIL ENGINEERING
COMMITTEE FOR CIVIL AND WATER ENGINEERING
POLISH ACADEMY OF SCIENCES ISSN 1230-2945
DOI: 10.24425/ace.2025.155099
ARCHIVES OF CIVIL ENGINEERING
Vol. LXXI ISSUE 3 2025
pp. 281 –294

Research paper

Simplifications of the numerical model in the design of bar and diaphragm bracing systems

Natalia Korcz-Konkol[1], Piotr Iwicki[2]

Abstract: The topic of transversal roof bracing design was discussed. The analysis was performed in ABAQUS for a part of the steel single-storey building roof consisting of truss girders and purlins. Structure with both diaphragm bracing (trapezoidal sheeting) and bar bracing was considered. Imperfection-origin forces (implemented using stabilising force) and wind loads were taken into account. Following modifications of the numerical model were analysed: substitution of the 3D shell model of the sheeting with an equivalent orthotropic shell, omission of the elasticity properties of the purlin-to-sheeting connection, omission of the eccentricity between purlins and sheeting. Influence of the simplifications of the numerical model on forces in bracing was assessed. Substitution of the 3D shell model of the sheeting with the equivalent orthotropic shell model with modification of the matrix stiffness according to the stressed skin theory gave more satisfactory results of the extreme forces in bar bracing than using "standard" stiffness matrix element values. What is more, the numeration simplification of the purlin-to-sheeting connection (omission of the connection flexibilities) affected the results less than the omission of the purlin-sheeting eccentricity.

Keywords: fastener, imperfection, orthotropic plate, roof bracing, stressed-skin effect, trapezoidal sheeting

[1]Sc., Eng., Gdańsk University of Technology, Faculty of Civil and Environmental Engineering, ul. Gabriela Narutowicza 11/12, 80-233 Gdansk, Poland, e-mail: natalia.korcz@pg.edu.pl, ORCID: 0000-0002-8775-2584
[2]DSc., Eng., Prof. GUT, Gdańsk University of Technology, Faculty of Civil and Environmental Engineering, ul. Gabriela Narutowicza 11/12, 80-233 Gdansk, Poland, e-mail: piwicki@pg.edu.pl, ORCID: 0000-0003-1652-2594

1. Introduction

In traditional design of the steel single-storey buildings only bar bracing is considered and the stiffening effect of the cladding on the structure resulting from the in-plane (shear) resistance and stiffness of the sheeting ("stressed skin effect", "diaphragm effect") is omitted. This approach is assumed to be safe and in most common cases it is true. However, the alarming phenomenon of the unwanted (undesired) stressed skin effect was noticed in existing structures, especially in big sheds, where leakage or even failure occurred [1–4]. Therefore it should be remembered that the diaphragm effect occurs, to a certain extent, even if it was not considered by the designer. On the other hand, the advantage of the interaction between structural elements and cladding may be used for construction optimisation [5,6]. Both trapezoidal sheets and sandwich panels can interact with the main structure and its elements, but taking this fact into account in the design requires a slightly different approach, resulting from the specific characteristics of both cladding systems [7,8]. This paper focuses on cladding made of trapezoidal sheeting.

According to [5] the shear flexibility of the diaphragm made of trapezoidal sheeting is related to the sum of the diaphragm components deformation. These elements of the diaphragms are: sheeting, connections and edge members. Sheeting deformation is due to profile distortion and shear strain. It is influenced not only by the diaphragm geometry but also by the location of the sheeting to purlin fasteners (in every or alternate troughs, central or side position in the trough [9]) and by the length of sheets. Depending on the roof structure (with or without purlins), different range of the connections are specified. For example, in roof with purlins following connections occurred: sheet to purlin fasteners, seam fasteners (sheet to sheet fasteners), purlin to rafter connections and shear connections (if exists). Additionally, the stressed-skin effect results in flange forces in the edge elements of the diaphragm. When wind acting on gable wall, the flange forces occurred in upper truss chords or rafters of the structure.

Nowadays numerical analysis of the entire structure is becoming more and more common in the design process. If a 3D numerical model built for the purpose of standard static calculations exists, it seems reasonable to use it also (after required modifications) for more specific goals. In view of the above, from the design point of view it is important and may be useful to know the methods of considering the diaphragm effect components in the numerical analysis. The issue is still the subject of ongoing research, e.g. [3, 10, 11] . Other example is the comparison between numerical design models, presented in [12, 13], in the context of the influence of the cladding on the stability of the structural elements. Simplifications of the numerical models of the trapezoidal cladding and connections were examined also in [9, 14, 15]. Despite the above, there is no clear answer how to build the numerical model of the structure with the stressed skin effect of the sheeting included. Commonly available numerical modelling tools are not fully verified in this respect. The more essential it is to be aware of the consequences of the simplifications of the numerical model on final results.

In this study the role of diaphragm stiffness is considered in the context of transverse roof bracing design. This is a continuation of a larger research task [16]. Detailed numerical models, while important for the scientific purposes, are not suitable for use in engineering practise. Therefore, the main objective of this research was to assess the influence of successive numerical model simplifications on the forces in bracing, as the issue which may be essential for the designers.

2. Materials and methods

2.1. Basic characteristic of the analysed structure

Part of the steel single-storey building roof consisting of truss girders and purlins with the combination of bracing systems (bar and diaphragm) was analysed. The structure is presented in Fig. 1.

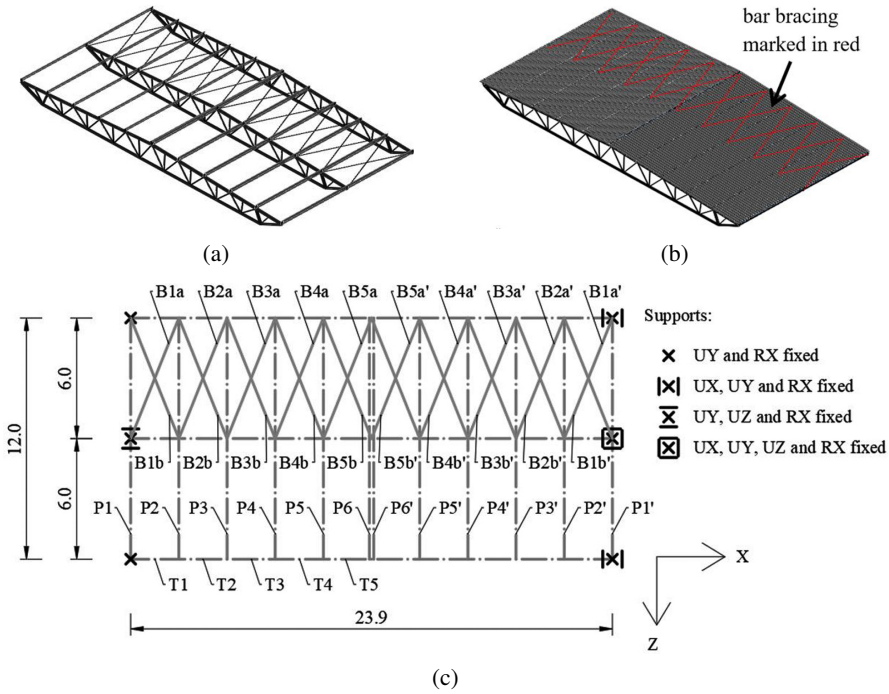

Fig. 1. Analysed structure: (a) general view (sheeting omitted for the clarity), (b) general view (bar bracing covered in a view by the sheeting – marked in red), (c) scheme of the truss supports with main dimensions and symbols of the main elements (P – purlins, T – upper truss chord elements, B – bar bracing members)

The model was built following the structure studied in [16]. Trusses with the span equal to 24 m were placed in 6 m distance. The trusses had non-uniform depth from 0.9 m at the supports to 1.61 m in the middle of the span. The truss chords were made of 2L profiles (upper chord – 2L90 × 90 × 9 profile and the bottom chord – 2L80 × 80 × 8 profile). The upper truss chord profiles were connected using 14 battens (180 × 74 × 5 mm plates) at midpoints between truss joints. Diagonals were made of U65 profile, except the diagonals close to the supports, which were made of 2L65 × 65 × 7 profile. Purlins were made of Z250 × 65 × 2 profiles and supported on the chords with 2.39 m spacing using angle cleats (L235 × 55 × 8, length – 0.165 m).

The transversal roof bracing was realised using X-shaped bracing made of flat bar bracing members (30 × 4 mm). Additionally, the trapezoidal sheeting was considered as a structural element and a part of the bracing system. The trapezoidal sheeting cross section is presented in Fig. 2. The fastening of the sheeting to the purlin was realised in every corrugation in the centreline of the bottom flange of the sheeting. In the analysed structure there were no shear connectors, which is a common practise.

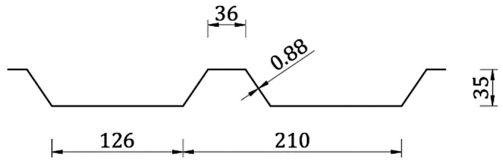

Fig. 2. The geometry of the trapezoidal sheeting cross-section [mm]

The following values were assessed: the yield strength of the steel f_y = 350 MPa, the modulus of elasticity E = 205 GPa and the Poisson's ratio in elastic stage ν = 0.3.

2.2. Detailed numerical model

Analysis was conducted in Abaqus software [17]. Detailed model from the previous analysis [16] was a starting model. Truss chords and diagonals, purlin-chord connectors and trapezoidal sheeting were applied as S4R shell elements (4-node shell with reduced integration). Purlins were applied as B31OS beam elements (2-node linear open-section beam). The axis of the purlin beam element was established in the middle of the web height. The eccentricity between purlins and other elements of the structure (truss, sheeting, bar bracing) were taken into account. Bar bracings were applied as B31 beam elements (2-node linear beam).

Truss elements (diagonals and chords) were connected using "Tie" connection between small end area of the particular elements. Connection between bar bracing and the truss was simplified using "Coupling" procedure (end nodes of bar elements were coupled to the central nodes of the angle cleats).

Purlins were connected to the trusses using angle cleats. Angle cleats were applied in numerical model as S4R shell elements. The horizontal part of every angle cleat was tied to the chord using shell to shell constraint. What is more, four nodes of the vertical part of every angle cleat, which mapped the group of bolts, were coupled to the corresponding node of the purlin. Thanks to use of shell elements, the main component of the purlin to sheeting connection flexibility, which is the flexibility of the angle cleat, was included. However, the purlin was built from B31OS beam elements, so the local effect of the connection upper flange of the purlin and bottom flange of the sheeting was omitted.

Finally, purlin-to-sheeting connections (screws) were modelled using bushing connector elements [17]. The connection elements were defined in the exact place of the screws – between nodes at the axis of the purlin and corresponding nodes on the bottom flange of the sheeting. Using bushing elements enable to include in the analysis the elasticity of the connection. Tension, bending and torsion elasticity properties (stiffnesses) were calculated based on the

geometry of the fastener. The shear stiffness (the stiffness in the plane of the diaphragm), which is the most important purlin-to-sheeting fastener elasticity component when considering the diaphragm effect, was calculated based on the theoretical slip s_p of the screw with neoprene washer, which, according to [5], was assessed equal to 0.35 mm/kN. Formulas used to calculate all elasticity values were presented in Table 1.

Table 1. Purlin-to-sheeting connection elasticity components

Fastener elasticity component	**Formula**	**Value**
Shear stiffness	$\frac{1}{s_p}$	2857 N/mm
Tension stiffness	$\frac{EA}{l} = \frac{E}{l} \cdot \frac{\pi d^2}{4}$	3382257 N/mm
Bending stiffness	$\frac{4EI}{l} = \frac{4E}{l} \cdot \frac{\pi d^4}{64}$	25.578 N·mm
Torsion stiffness	$\frac{GI_s}{l} = \frac{E}{2(1+\upsilon)l} \cdot \frac{\pi d^4}{32}$	4.919 N·mm
where: s_p – slip per sheet/purlin fastener per unit load according to [5], l – the length of the screw measured between the central axis of the connected elements, d – the diameter of the screw.		

The assemble process of the sheets was not taken into account – the trapezoidal sheeting was treated as one structural element, seam fasteners were omitted in the analysis. It means that the length of particular sheets was not reflected, nor was the flexibility of seam fasteners.

2.3. Load scheme of the analysed structure

In the transverse roof bracing design it is required to considered not only the external loads (such as wind loads), but also the stabilising forces due to the initial imperfection of the restrained elements (upper truss chords).

Selected analytical and numerical methods of taking into account the imperfections of the truss girder were compared in [16, 18], where three variants of roof bracing (bar bracing, diaphragm bracing and the combination of bar and diaphragm bracing) and different shapes of the imperfection were considered. In this study, imperfections of the chosen truss (the gable one, bottom in Fig. 1) were implemented using the Eurocode 3 procedure [19]. The equivalent stabilising force q was calculated according to [19], then, applied in the numerical model along the upper truss chord.

Additionally wind acting on gable wall was taken into account. Wind load was applied to the centre points of the purlin-chord connectors as point loads with the value $W = 7.65$ kN (and $W/2 = 3.82$ kN at the eave joints). The value of the reactions from the gable column to the roof corresponded to the wind load equal to 0.8 kN/m^2 and the average height of the gable wall equal to 8 m. The load scheme is presented in Fig. 3.

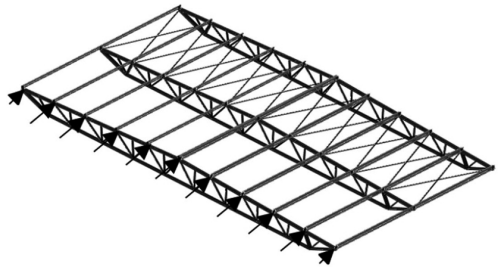

Fig. 3. Wind loads scheme (sheeting omitted for the clarity)

2.4. Simplifications of the numerical model

Detailed numerical model described in Section 2.1 was a starting model for the analysis. Then, numerical model was modified according to the schedule presented in Table 2. The method of assigning symbols to subsequent models is explained in Fig. 4.

Table 2. Characteristic of the simplified numerical models of the roof

Symbol of model	Trapezoidal sheeting	Purlin/sheet fasteners	Purlin/sheet eccentricity
T_F1_O (starting model)	shell	bushing	+
T1_F1_O	ortho_1	bushing	+
T2_F1_O	ortho_2		
T3_F1_O	ortho_3		
T1_F2_O	ortho_1	coupling	+
T1_F2_WO			–
T2_F2_O	ortho_2	coupling	+
T2_F2_WO			–

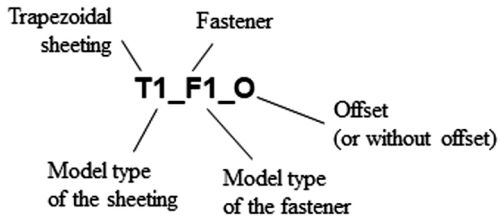

Fig. 4. Explanation of assigning symbols to numerical models of the roof

First of all, modifications were based on a substitution of the 3D shell model of the sheeting (see Fig. 5a) with an equivalent orthotropic shell. The substitution of the corrugated sheeting with an orthotropic shell (or plate) model is frequently used engineering procedure which

enable to simplify the numerical model of the structure and simultaneously include the most important characteristic of these elements. Popular approach is to approximate corrugated panel by an orthotropic classical Kirchhoff plate with the ignoring the coupling stiffness matrix, which gives following constitutive equation [20]:

$$\begin{bmatrix} N_x \\ N_y \\ N_{xy} \\ M_x \\ M_y \\ M_{xy} \end{bmatrix} = \begin{bmatrix} D_{11} & D_{12} & 0 & 0 & 0 & 0 \\ D_{12} & D_{22} & 0 & 0 & 0 & 0 \\ 0 & 0 & D_{33} & 0 & 0 & 0 \\ 0 & 0 & 0 & C_{11} & C_{12} & 0 \\ 0 & 0 & 0 & C_{12} & C_{22} & 0 \\ 0 & 0 & 0 & 0 & 0 & C_{33} \end{bmatrix} \cdot \begin{bmatrix} \varepsilon_x \\ \varepsilon_y \\ \gamma_{xy} \\ \kappa_x \\ \kappa_y \\ \kappa_{xy} \end{bmatrix} \tag{2.1}$$

where: x, y – orthogonal in-plane coordinates, N_x, N_y, N_{xy} – membrane forces, M_x, M_y, M_{xy} – flexural moments, $\varepsilon_x, \varepsilon_y, \nu_{xy}$ – membrane strains, K_x, K_y, K_{xy} – curvature strains, D, C – membrane (extensional/shear) and flexural (bending/torsional) stiffness matrix.

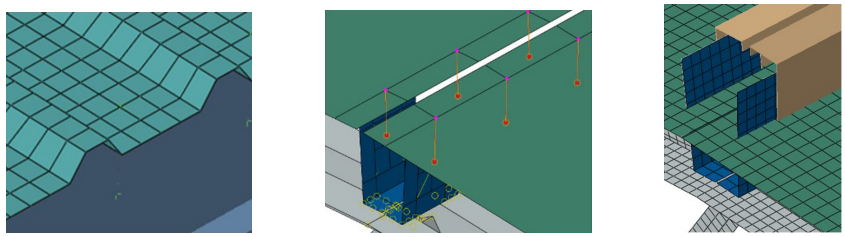

(a) (b) (c)

Fig. 5. Details of the simplified numerical model of the roof: (a) 3D shell model of the trapezoidal sheeting, (b) coupling connections (models "F2") between purlin and sheeting with the eccentricity included, (c) orthotropic shell in the axis of the purlin (models without the eccentricity "WO")

Different formulas for equivalent orthotropic stiffness matrix elements for trapezoidal sheeting are given in the literature [5, 21–25]. In [14, 15] the comparison of the selected formulas was already presented in the context of the stressed-skin design – based on the analysis of the flexibility of the cantilevered diaphragm and based on the global deflections of the structure loaded by the wind acting on longitudinal wall. In this study the case of the roof loaded by the wind acting on gable wall is analysed. Three approaches to calculate the stiffness matrix elements were chosen to consideration. In Table 3. formulas for the stiffness matrix elements of the equivalent orthotropic plate were presented, which is commented below in more details. Trapezoidal sheeting was built using the General Stiffness Section [17], which allowed to define extensional and bending rigidities. The values of the stiffness matrix elements obtained for the trapezoidal sheeting in the analysed structure were presented in Table 4.

In "Ortho_1" case, the "standard" stiffness matrix elements was used [25]. It is the example of the approach implemented in one of the engineering software dedicated to the static analysis of the structures. One aspect requires extra comment: in formula for D_{11} according to [25], where specific formulas derived for trapezoidal sheeting based on [20] were presented, the

Table 3. Analytical formulas for stiffness matrix of equivalent orthotropic plate

Stiffness matrix element	**Ortho_1**	**Ortho_2**	**Ortho_3**
Extensional rigidities [kN/m]			
D_{11}	$\dfrac{d}{\dfrac{I_1\left(1-\nu^2\right)}{Et}+\dfrac{12I_2\left(1-\nu^2\right)}{Et^3}}$		$E\cdot\dfrac{I_y^0}{I_y}$
D_{12}	$\nu\cdot D_{11}$		$\nu\cdot D_{11}$
D_{22}	$\nu\cdot D_{12}+\dfrac{u}{d}\left(\nu-\nu^2\right)\dfrac{Et}{1-\nu^2}$		$\nu\nu\dfrac{Et}{1-\nu_{xy}\cdot\nu_{yx}}\cdot\dfrac{u}{d}$
D_{33}	$\dfrac{d}{u}\cdot\dfrac{Et}{2(1+\nu)}$	$\dfrac{a}{b\cdot(c_{1.1}+c_{1.2})}$	
Flexural (bending) rigidities [kN·m]			
C_{11}	$\dfrac{d}{u}\cdot\dfrac{Et^3}{12(1-\nu^2)}$		$\dfrac{d}{u}\cdot\dfrac{Et^3}{12}$
C_{22}	$\dfrac{1}{d}\left[I_2\dfrac{Et}{1-\nu^2}+I_1\dfrac{Et^3}{12\left(1-\nu^2\right)}\right]$		$E\cdot\dfrac{I_{y,0.5}}{d}$
C_{33}	$\dfrac{u}{d}\cdot\dfrac{Et^3}{24(1+\nu)}$		$\dfrac{Et^3}{12(1+\nu)}$

Symbols are explained in Fig. 6. and in the text. Additionally:
t – the thickness of trapezoidal sheeting (and, as assumed, thickness of equivalent orthotropic plate),
I_y^0 – equivalent plate moment of inertia,
I_y – trapezoidal plate section moment of inertia,
a, b – dimensions of the shear panel,
$c_{1,1}$, $c_{1,2}$ – flexibility components according to [5],
$I_{y,0.5}$ – moment of inertia of the half of the corrugation.
Complementary formulas:

$$I_1 = d - 2h\frac{\cos(90^\circ-\Theta\,(1-\cos(90^\circ-\Theta))}{\sin\Theta}$$

$$I_2 = \frac{2\left((h-y_0)^3+y_0^3\right)}{3\sin(90^\circ-\Theta)} + l_1\,(h-y_0)^2 + 2l_2y_0^2$$

$$y_0 = \frac{l_1 h}{u} + \frac{h^2}{u\sin(90^\circ-\Theta)}$$

$$\underset{\nu_{xy}\,=\,\nu}{}$$

$$\nu_{yx} = \nu\cdot E_{yy}/E_{xx}$$

$$\frac{I_y^0}{I_y} = \frac{t^3}{12}\cdot\frac{d}{I_2\cdot t} = \frac{d}{\dfrac{12I_2t}{t^3}}$$

$$I_{y,0.5} = \frac{tI_2}{2}$$

where:
l_1, l_2 – width of the flange of the sheeting (top and bottom respectively).

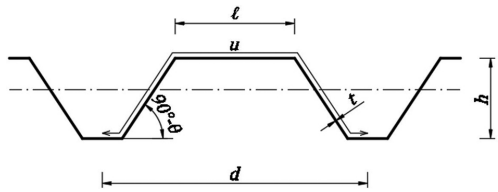

Fig. 6. Trapezoidal sheeting geometry – symbols used in Table 3

Table 4. Element values of stiffness matrix of equivalent orthotropic shell

Stiffness matrix element	**Ortho_1**	**Ortho_2**	**Ortho_3**
	Extensional rigidities [kN/m]		
D_{11}	55.69		50.69
D_{12}	16.71		15.21
D_{22}	233058		212083
D_{33}	59021	7496	
Flexural (bending) rigidities [kN·m]			
C_{11}	0.011		0.010
C_{22}	45.54		41.43
C_{33}	0.005		0.009

component $(\nu - \nu^2)$ was given, causes that the D_{11} element differs significantly from the results according to other procedures. Based on the analysis of the formula and comparison with alternative methods, component $(\nu - \nu^2)$ was considered questionable and the calculations were carried out omitting it.

When the diaphragm effect is under consideration, modifications of the stiffness matrix are suggested to include in the calculations factors important in case of stressed skin effect [10, 26, 27]. Then, in order to take into account the stressed-skin theory, in case of "Ortho_2" and "Ortho_3" models, components of shear flexibility due to sheet deformation (due to profile distortion – $c_{1.1}$ and shear strain – $c_{1.2}$ according to [5] were used to calculate the D_{33} value of extensional rigidity [10, 26]. In "Ortho_1" model element D_{33} is dependent on cross-section geometry of the trapezoidal sheeting and material properties only, while the shear flexibility is more complex issue. In case of "Ortho_2" and "Ortho_3" models much more data were taken into account. In particular, flexible component $c_{1.1}$ (the result of profile distortion) depends not only on the sheet geometry but also among others on the way of sheet/purlin fastening (in every corrugation/in every double corrugation) and on the number of sheets in the width of the panel assembly. Value of shear flexibility may be determined experimentally/ numerically/ analytically. In this study, calculation of the shear flexibility components $c_{1.1}$ and $c_{1.2}$ was made according to [5]. Taking into account the static scheme of the roof panel

in the context of the considered loads (loads in the direction perpendicular to the gable wall and non-continuity of the sheeting in the ridge), case of cantilevered diaphragm with sheeting spanning parallel to the length of the diaphragm was identified. Components were modified by the multiplier b^2/a^2 in order to gain the flexibility in a direction perpendicular to the corrugations. Then, D_{33} component was calculated for the following data: $a = 6$ m, $b = 12$ m, $(c_{1.1} + c_{1.2}) = 0.0667$ mm/kN, where a, b are the dimensions of the shear panel.

Finally, in "Ortho_3" model, different formulas for all matrix elements except D_{33} were used: extensional rigidities were calculated based on [10,26], then flexural (bending) rigidities – based on [28], where the combination of two approaches [22,23] was suggested. The analysis of the approaches to calculate the equivalent orthotropic matrix showed that the procedures differ in particular assumptions, e.g. according to [23] $1 - \nu^2 \approx 1$ may be assumed in calculations of C_{11} and C_{22}, while other approaches consider Poisson's ratio influence. Equations for bending stiffness elements C_{11} and C_{22} according to [23] is also confirmed based on [5] and the assumption $1 - \nu^2 \approx 1$. In all cases it was included that – for corrugated sheeting – the Poisson's ratio $\nu_{xy} = \nu$, which means that it is the same as that of the isotropic material [28]. In [10,27] it was assumed again, that the Poisson's ratio $\nu_{xy} = \nu$, and – additionally to other approaches – that $\nu_{yx} = \nu \cdot E_{yy}/E_{xx}$. In fact, "Ortho_3" model was created only for one goal – to confirm the assumption that the minor differences between matrix elements (9% for most values except C_{33} – see Table 4) have little effect on the results.

In the next group of variants, purlin-to-sheeting connection was simplified by using a coupling connection with six degrees of freedom fixed and no elasticity defined instead of a bushing connection. Two of the analysed orthotropic models of the sheeting were considered (T1_F2_O and T2_F2_O). Connection was defined between the pairs of nodes, (see Fig. 5b), so the number of the fasteners and the distance between them were included (but not the position relative to the cross-section of corrugations, as the cross-section, due to use the orthotropic shell, was modelled as "smeared").

Finally, the issue of eccentricities was examined. The eccentricity between purlin and sheeting, which in the previous models corresponded to the real positions of the elements, was omitted. The orthotropic shell was placed in the axis of the purlins, as shown in Fig. 5c. The eccentricity analysis was performed for the purlin-to-sheeting connection variant, again with the use of coupling elements. This approach illustrates the behaviour of the structure in the numerical model when the only flexibility of the diaphragm considered is the flexibility of the truss-purlin connection. Analysis was performed for two orthotropic models (T1_F2_WO and T2_F2_WO).

3. Results and discussion

All variants were compared in terms of axial forces in bar bracing as a measure of the force distribution between bar and diaphragm bracing. Results are presented in Fig. 7, with the exception of the T3_F1_O model (sheeting as Ortho_3 model, fasteners as bushing elements, eccentricity included). The T3_F1_O model was used for comparison only, to test how minor differences in matrix elements (9% for most values except C_{33} – see Table 4) affect the results. It turned out that the differences in the results of forces in bar bracings did not exceed 2.5%,

which confirms that changes in stiffness elements other than D_{33} have little effect on the force distribution in the structure.

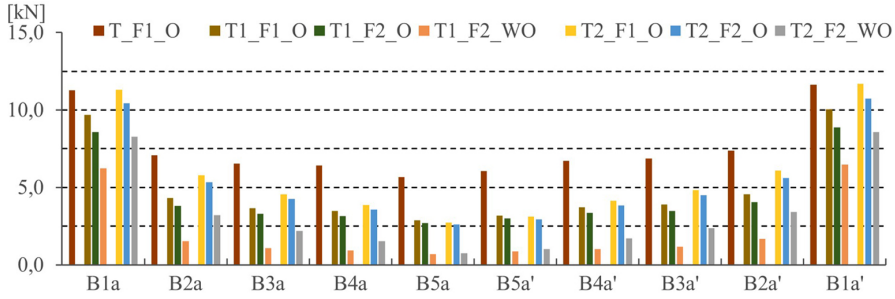

Fig. 7. Axial forces in bar bracing elements

The observations regarding the remaining variants of the models were as follows:

- using "standard" stiffness matrix elements for the modelling of the equivalent orthotropic shells (Ortho_1 model, e.g. in T1_F1_O) led to a 14% reduction of the extreme forces in bar bracing, which means that the sheeting bore more stress than the shell model (T_F1_O) of the sheeting implied,
- modification of the D_{33} element of the matrix stiffness according to the stressed skin theory (Ortho_2 model, e.g. in T2_F1_O) got us closer to the result obtained for the shell model (T_F1_O) – very high consistency of the results of extreme force in bar bracing was obtained (0.5% difference),
- for bar bracing elements closer to the midspan of the transverse bracing system, the differences between orthotropic models were decreased, in particular in the area of the ridge the difference was barely noticeable; it was due to the fact that in that area the sheeting was barely under shear,
- the numeration simplification of the purlin-to-sheeting connection (omission of the connection flexibilities) showed up the most in the side bar elements (the closest ones to the side wall) where 8–12% reduction of the forces was noticed compared to the corresponding orthotropic model with the flexibility of the connections taken into account; this gave in total up to 24% reduction of extreme forces in bar bracing in T1_F2_O model compared to the shell model (T_F1_O),
- the omission of the purlin-sheeting eccentricity resulted in a 21-27% reduction of the extreme forces in bar bracing compared to the corresponding orthotropic model with the eccentricity taken into account; this gave in total up to 45% reduction of extreme forces in bar bracing in the T1_F2_WO model compared to the shell model (T_F1_O).

For each case, the maximum horizontal displacements in the direction of the loading were also observed in the ridge of the end truss. The results are summarized in Table 5 together with the extreme values ??of forces in bar bracing. The simplifications of the model (bushing fastener replaced by coupling, omission of the eccentricity) caused the decrease of the displacements (as the next flexibilities were omitted). The biggest decrease was due to the omission of the eccentricity between the purlin and the sheeting – 63% reduction in T1_F2_WO model

compared to the shell model (50% reduction in case of T2_F2_WO model) and 43% reduction compared to T1_F2_O model (34% in case of T2_F2_O model). What is more, the decrease in the displacements followed the decrease in the extreme forces in bar bracing.

Table 5. Maximal horizontal displacements (UZ) and extreme axial forces in bar bracing obtained in the analysis of the simplified numerical model of the roof

Model	UZ [mm]	FX [kN]
T_F1_O	–15.6	11.6
T1_F1_O	v11.0	10.0
T1_F2_O	v10.0	8.9
T1_F2_WO	v5.7	6.5
T2_F1_O	v12.5	11.7
T2_F2_O	–11.7	10.7
T2_F2_WO	–7.8	8.6

Analysis was performed for the case of the structure with both bar and diaphragm bracing system (BDBr). As there were two components of transverse bracing system (bar and diaphragm), the reduction of the bar bracing forces was related to the stresses increase in the sheeting. Thus, the relationship between the simplification of the numerical model and the change in the force distribution in the structure was established.

4. Conclusions

Numerical research of the purlin roof bar and diaphragm bracing including imperfection-origin forces and wind loads were presented. Simplifications of the numerical model were introduced in order to assess their influence on forces in bracing. The results were discussed in Section 3. The main conclusions are as follows:

– substitution of the 3D shell model of the sheeting with the equivalent orthotropic shell model with modification of the D_{33} element of the matrix stiffness according to the stressed skin theory gives more satisfactory results of the extreme forces in bar bracing than using “standard” stiffness matrix element values,
– the numeration simplification of the purlin-to-sheeting connection (omission of the connection flexibilities) affects the results less than the omission of the purlin-sheeting eccentricity.

Seam fasteners were not considered. What is more, purlins were built from beam elements, so the torsional deformation of the purlin (due to the local effect of the connection of the upper flange of the purlin and bottom flange of the sheeting) was the issue omitted in the analysis. Further research for verification and generalising the results is needed. However, the above observations are preliminary guidelines for numerical analysis of the roof structure in the design of bar and/or diaphragm bracing.

Acknowledgements

The numerical calculations were performed using the computing resources of CI TASK at Gdańsk University of Technology.

References

[1] J.M. Davies, M.J. Roberts, and Y.C. Wang, "Stressed skin theory and structure cladding interaction: Safety concerns with Big Sheds", *Thin-Walled Structures*, vol. 169, art. no. 108415, 2021, doi: 10.1016/j.tws.2021.108415.

[2] M.J. Roberts, J.M. Davies, and Y.C. Wang, "Modern cladding systems for big sheds: The emerging state of the art", *Thin-Walled Structures*, vol. 175, art. no. 109264, 2022, doi: 10.1016/j.tws.2022.109264.

[3] M. Roberts and J.M. Davies, "3D models of clad steel structures – Assumptions and validation", in *Current Perspectives and New Directions in Mechanics, Modelling and Design of Structural Systems: Proceedings of The Eighth International Conference on Structural Engineering, Mechanics and Computation, 5–7 September 2022, Cape Town, South Africa*. CRC Press, 2022, doi: 10.1201/9781003348443.

[4] M.J. Roberts, J.M. Davies, and Y.C. Wang, "Numerical analysis of a clad portal frame structure tested to destruction", *Structures*, vol. 33, pp. 3779–3797, 2021, doi: 10.1016/j.istruc.2021.06.098.

[5] ECCS, *European Recommendations for the Application of Metal Sheeting Acting as a Diaphragm. Stressed Skin Design*. European Convention for Constructional Steelwork, 1995.

[6] ECCS, *European Recommendations on the Stabilization of Steel Structures by Sandwich Panels*. European Convention for Constructional Steelwork, 2014.

[7] Z. Nagy, B.-A. Lőrincz, A. Kelemen, G. Zsongor, and A. Sánduly, "Experimental investigations on diaphragms made of sandwich panels and corrugated sheets", presented at Ninth International Conference on Thin-Walled Structures – ICTWS2023, 29 November–1 December 2023, Sydney, Australia, 2024.

[8] K. Ciesielczyk and R. Studziński, "Experimental investigation of sandwich panels supported by thin-walled beams under various load arrangements and number of connectors", *Archives of Civil Engineering*, vol. 68, no. 4, pp. 389–402, 2022, doi: 10.24425/ace.2022.143045.

[9] N. Korcz-Konkol and E. Urbańska-Galewska, "Influence of sheet/purlin fasteners spacing on shear flexibility of the diaphragm", *MATEC Web of Conferences*, vol. 219, art. no. 02007, 2018, doi: 10.1051/matecconf/201821902007.

[10] M. Gryniewicz and J.K. Szlendak, "FEM model of the steel building roof includes stressed skin diaphragm action effects", in *Proceedings of the XIII International Conference on Metal Structures: ICMS 2016*. CRC Press, 2016, pp. 93–100.

[11] M. Gryniewicz, M.J. Roberts, and J. M. Davies, "Testing and analysis of a full-scale steel-framed building including the consideration of structure-cladding interaction", *Journal of Constructional Steel Research*, vol. 181, art. no. 106611, 2021, doi: 10.1016/j.jcsr.2021.106611.

[12] Z. Nagy, A. Pop, I. Mois, and R. Ballok, "Stressed Skin Effect on the Elastic Buckling of Pitched Roof Portal Frames", *Structures*, vol. 8, pp. 227–244, 2016, doi: 10.1016/j.istruc.2016.05.001. The numerical calculations were performed using the computing resources of CI TASK at Gdańsk University of Technology.

[13] Z. Nagy, A. Kelemen, and M. Nedelcu, "The influence on portal frame buckling of different cladding systems – A comparative numerical study considering stressed skin effect", *Thin-Walled Structures*, vol. 182, 2022, doi: 10.1016/j.tws.2022.110310.

[14] N. Korcz, "Modele numeryczne uwzględniające tarczową pracę pokrycia dachowego z blach trapezowych", *Czasopismo Inżynierii Lądowej, Środowiska i Architektury / Journal of Civil Engineering, Environment and Architecture*, vol. 64, no. 4/I, pp. 213–228, 2017, doi: 10.7862/rb.2017.207.

[15] N. Korcz and E. Urbańska-Galewska, "Influence of fasteners and connections flexibility on deflections of steel building including the stressed skin effect", *Technical Sciences / University of Warmia and Mazury in Olsztyn*, vol. 21, no. 2, pp. 131–148, 2018, doi: 10.31648/ts.2722.

[16] N. Korcz-Konkol and P. Iwicki, "Truss imperfections in the design of bar and diaphragm bracing systems", *Journal of Constructional Steel Research*, vol. 206, art. no. 107936, 2023, doi: 10.1016/j.jcsr.2023.107936.

[17] ABAQUS, *Abaqus Documentation 2021*. Dassault systèmes SIMULIA Corp., 2021.

[18] N. Korcz-Konkol and P. Iwicki, "Stabilizing forces in trapezoidal sheeting used as a part of the bracing system", *ce/papers*, vol. 4, no. 2–4, pp. 2242–2248, 2021, doi: 10.1002/cepa.1545.

[19] EN 1993-1-1 Eurocode 3: Design of steel structures – Part 1–1: General rules and rules for buildings. CEN, 2005.

[20] Y. Xia, M.I. Friswell, and E.I.S. Flores, "Equivalent models of corrugated panels", *International Journal of Solids and Structures*, vol. 49, no. 13, pp. 1453–1462, 2012, doi: 10.1016/j.ijsolstr.2012.02.023.

[21] PN-EN-1993-4-1 Eurokod 3. Projektowanie konstrukcji stalowych. Część 4-1: Silosy. PKN, 2009.

[22] D. Briassoulis, "Equivalent orthotropic properties of corrugated sheets", *Computers & Structures*, vol. 23, no. 2, pp. 129–138, 1986, doi: 10.1016/0045-7949(86)90207-5.

[23] A. Samanta and M. Mukhopadhyay, "Finite element static and dynamic analyses of folded plates", *Engineering Structures*, vol. 21, no. 3, pp. 277–287, 1999, doi: 10.1016/S0141-0296(97)90172-3.

[24] K.M. Liew, L.X. Peng, and S. Kitipornchai, "Buckling analysis of corrugated plates using a mesh-free Galerkin method based on the first-order shear deformation theory", *Computational Mechanics*, vol. 38, no. 1, pp. 61–75, 2006, doi: 10.1007/s00466-005-0721-2.

[25] Z. Ma, J. Havula, K. Mela, and J. Kesti, "Structural Fire Analysis of One-storey Steel-framed Buildings with Steel Claddings", *ce/papers*, vol. 4, no. 2–4, pp. 1213–1222, 2021, doi: 10.1002/cepa.1414.

[26] J. Bródka, R. Garncarek, and K. Miłaczewski, *Blachy fałdowe w budownictwie stalowym*. Warszawa: Arkady, 1999.

[27] M. Gryniewicz and J. Szlendak, "Wpływ współpracy pokrycia dachowego na przemieszczenia konstrukcji hali stalowej", *Inżynieria i Budownictwo*, vol. 72, no. 8, pp. 431–434, 2016.

[28] D. Wennberg, P. Wennhage, and S. Stichel, "Orthotropic Models of Corrugated Sheets in Finite Element Analysis", *ISRN Mechanical Engineering*, vol. 2011, art. no. 979532, 2011, doi: 10.5402/2011/979532.

Uproszczenia modelu numerycznego w projektowaniu stężeń prętowych i tarczowych

Słowa kluczowe: blacha trapezowa, imperfekcje, łączniki, płyta ortotropowa, stężenie dachowe, współpraca tarczowa

Streszczenie:

Poruszono temat projektowania poprzecznych stężeń dachowych. Analizę przeprowadzono w programie ABAQUS dla fragmentu stalowego dachu budynku jednokondygnacyjnego składającego się z dźwigarów kratowych i płatwi. Rozważono konstrukcję zawierającą zarówno stężenia tarczowe (blacha trapezowa), jak i stężenia prętowe. Uwzględniono siły powstałe w wyniku imperfekcji (za pomocą siły stabilizującej) oraz obciążenie wiatrem. Analizie poddano następujące modyfikacje modelu numerycznego: zastąpienie trójwymiarowego modelu powłokowego poszycia zastępczą powłoką ortotropową, pominięcie podatności połączenia płatwi z blachą, pominięcie mimośrodu pomiędzy płatwiami i poszyciem. Oceniono wpływ uproszczeń modelu numerycznego na siły występujące w stężeniu prętowym. Zastąpienie trójwymiarowego modelu powłokowego poszycia powłoką ortotropową z modyfikacją macierzy sztywności zgodnie z teorią współpracy tarczowej dało bardziej zadowalające wyniki ekstremalnych sił w stężeniu prętowym niż zastosowanie „standardowych" wartości elementów macierzy sztywności. Co więcej, uproszczenie w modelu numerycznym połączenia płatwi z blachą (pominięcie podatności połączenia) wpłynęło na wyniki w mniejszym stopniu niż pominięcie mimośrodu płatwi.

Received: 2024-05-10, Revised: 2024-06-03